ELECTRONIC, OPTICAL AND MECHANICAL PROPERTIES OF GRAPHENE/MoS_2 NANOCOMPOSITE

Nguyen Van Chuong[1,*], Nguyen Dinh Chien[1], Le Minh Duc[1], Nguyen Ngoc Hieu[2], Nguyen Son Tung[3]

[1]Le Quy Don Technical University;
[2]Duy Tan University;
[3]Hanoi University of Industry

Abstract

In this work, we construct an ultrathin graphene/MoS_2 nanocomposite and investigate systematically its electronic, optical and mechanical properties using first-principles calculations based on density functional theory. Our results show that graphene and MoS_2 layers in their corresponding graphene/MoS_2 nanocomposite are bonded mainly via the weak van der Waals forces, which are not enough to modify the intrinsic properties of the constituent monolayers, thus the electronic properties are well preserved. Moreover, the optical and mechanical properties of the graphene/MoS_2 nanocomposite are enhanced as compared with those of individual constituent graphene and MoS_2 monolayers. The maximum of absorption intensity can reach up to 2.5×10^5 cm^{-1}. Moreover, the Young's modulus of nanocomposite increases up to 487.2 N/m^2. These findings demonstrate that the formation of the graphene/MoS_2 nanocomposite could effectively be used to enhance the electronic, optical and mechanical performances of both graphene and MoS_2 monolayers.

Keywords: *Graphene/MoS_2 nanocomposite; two-dimensional materials; DFT calculations.*

1. Introduction

Since the discovery in 2004 by Geim and co-workers, graphene [1] has become one of the materials that have attracted both theoretical and experimental scientists due to its extraordinary physical properties. However, the application of graphene to technology, especially in the field of electronic and optoelectronic devices, still faces certain difficulties, in which the cause may be due to graphene having zero energy gap [2] and incompatibility between graphene and silicon electronic components. So far, there are many different ways to change the electronic states of graphene, i.e., to open the energy gap near the Fermi level in graphene: (i) the size effect leads to the opening of the energy gap in the nanoribbons; (ii) lateral effects and defects; (iii) doping and functionalism effects: spurious and functional atoms can change the material properties; (iv) layer (thickness) effect: the electronic structure depends strongly on the number of layers.

[*] Email: chuong.vnguyen@lqdtu.edu.vn

In parallel with finding a way to overcome this limitation of graphene, a new research direction has emerged strongly in the last five years. That is looking for alternative materials. This new research has focused on 2D materials such as phosphorene, antimonene, transition metal dichalcogenides (TMDs), and monochalcogenides, etc. Unlike graphene, these 2D materials are semiconductors with interesting properties and they become a potential candidate for applications in nanotechnology, such as photodetectors [3, 4], field effect transistors (FETs) [5],… These application potentials have prompted scientists to continue to study the outstanding electronic and transport properties of these materials and to explore their application potential for designing high-performance optoelectronic nanodevices.

An another method currently being investigated is the creation of vdW layered nanocomposites from 2D materials, thereby allowing for a better control of the electronic and mechanical properties of the constituent monolayers. Nanocomposites of 2D materials are stacked to create large electric fields originating from the difference in work function. Previously, Qiu and co-workers have investigated the optical properties of graphene/MoS_2 heterostructure by using the density functional theory [6]. Also, the mechanical properties of graphene/MoS_2 heterostructure have been studied by molecular dynamics simulations [7]. In addition, experimental and theoretical studies have shown that the extraordinary electronic properties of the constituent materials are preserved due to the weak vdW interaction between layers in the nanocomposites. First of all, we can mention the successful hybridization between graphene and a variety of other 2D semiconductor materials such as graphene/MoS_2 [8, 9], graphene/phosphorene [10], graphene/GaSe [11], etc. using different methods both experimentally and theoretically. Besides, hybridization between two-dimensional materials such as arsenene/C_3N [12], GaS/MoS_2 [13] is increasingly being considered. It can be seen that in these vDW nanocomposites, researchers have discovered some interesting properties that do not exist in individual constituent monolayers. For vdW nanocomposites, the vdW interactions between monolayers can keep the system stable even though the vdW interaction is very weak and this vdW force has little effect on the electronic properties around the Fermi level. These above studies show the great potential applications of monolayer 2D materials and their vdW nanocomposites in future nanodevices.

Therefore, in this work, we construct an ultrathin graphene/MoS_2 nanocomposite and systematically investigate its structural, electronic, optical and mechanical properties using first-principles calculations based on density functional theory (DFT). Our findings provide an opportunity for graphene/MoS_2 nanocomposite in the next-

generation nanoelectronic and optoelectronic devices, which could use to replace traditional silicon-based devices.

2. Computational models and methods

In the present work, we study the structural, electronic, and mechanical properties of the graphene and MoS_2 monolayer through first-principles calculations based on DFT. This method recently is encoded in the simulation QUANTUM ESPRESSO software [14]. The electron-ion interaction and the exchange-correlation energy were described by the projected augmented wave (PAW) method and generalized gradient approximation (GGA) within the Perdew-Burke-Ernzerhof (PBE) functional [15], respectively. All the geometric optimization and electronic properties calculations were performed with kinetic energy cut-off for wavefunctions of 35 Ry and for charge density of 350 Ry, respectively. Moreover, to describe the weak interactions, encapsulating in layered materials, we use the dispersion corrected DFT-D2 method [16]. The dipole correction has also been added in all calculations. The geometric optimization is performed within the energy and force convergence of 10^{-6} eV and 10^{-3} eV/Å, respectively. A 9×9×1 Monkhorst-Pack *k*-point mesh in the Brillouin zone (BZ) was used in all our GGA-PBE. A large vacuum thickness of 30 Å is employed to separate the spurious interactions between the periodic images.

Over the past ten years, many schemes have been proposed for incorporating vdW interactions into DFT calculations, such as non-local van der Waals density functional (vdW-DF) scheme proposed by Dion and semi-empirical long-range dispersion correction (DFT-D) proposed by Grimme. In this work, we have used DFT-D2 method to describe the weak interaction, which dominated between Graphene and MoS_2 monolayers. The advantage of DFT-D method is its simplicity, reliability and stability. Our calculations and the calculations of other groups show that for layered vdW heterostructures, the DFT-D scheme predicts the correct results. Therefore, we chose this scheme to consider the weak interaction in the G/MoS_2 vdWH owing to its reliability and stability. In addition, in my view, both non-local van der Waals density functional scheme and semi-empirical long-range dispersion correction work well for layered vdW heterostructures [17-19]. The vdW-DF slightly understated lattice parameter values, and DFT-D slightly overestimated. Generally, the results were similar. It can be assumed that when using the vdW-DF scheme, the distance will be slightly smaller, and the binding energy is slightly larger. In the DFT-D2 method, the total energy of system can be obtained by: $E_{tot} = E_{KS-DFT} + E_{disp} = E_{KS-DFT} + E_{vdW}$, where $E_{KS\text{-}DFT}$ is the total energy of systems by Kohn-Sham formula, and E_{disp} is the dispersion corrected total energy that includes the weak vdW forces and it can be calculated as follows [16]:

$$E_{disp} = -\frac{1}{2}\sum_{ij} C_{6ij}\left[\sum_{\vec{R}}\left|\vec{r}_{ij}+\vec{R}_{ij}\right|^{-6} f_{damp}\left(\left|\vec{r}_{ij}+\vec{R}_{ij}\right|\right)\right] \quad (1)$$

$$f_{damp}\left(\left|\vec{r}_{ij}+\vec{R}_{ij}\right|\right) = s_6\left\{1+\exp\left[-d\left(\frac{\left|\vec{r}_{ij}+\vec{R}_{ij}\right|}{r_0}-1\right)\right]\right\}^{-1} \quad (2)$$

3. Results and discussion

Tab. 1. Optimized lattice constant a (Å) and bond lengths d (Å) of freestanding graphene and MoS_2 and graphene/MoS_2 nanocomposite. Interlayer distance D between graphene and MoS_2 in nanocomposite is presented in the last column.

Materials	*a*	$d_{C–C}$	$d_{Mo–S}$	*D*
Graphene	2.461	1.425	-	-
MoS_2	3.183	-	2.410	-
Graphene/MoS_2	12.518	1.387	2.415	3.43

Before constructing the graphene/MoS_2 nanocomposite, we check the lattice constants of both graphene and MoS_2 monolayers at the ground state. Our calculated lattice constants of graphene and MoS_2 are 2.461 Å and 3.183 Å, respectively, which are in good agreement with previous theoretical and experimental reports [20-23]. It demonstrates that our calculated methods used in this work are reliabe. We further construct the atomic structure of graphene/MoS_2 nanocomposite by stacking graphene above on top of MoS_2 monolayer. The optimized lattice parameters of the graphene/MoS_2 nanocomposite are listed in Tab. 1. Due to large difference in the lattice constants between graphene and MoS_2, thus, to built the graphene/MoS_2 nanocomposite, we use a large supercell, containing of (5×5) unit cells of graphene and (4×4) unit cells of MoS_2 monolayer. The overall lattice mismatch in the graphene/MoS_2 nanocomposite is calculated to be 3.08%, which insignificantly affects the main results. The atomic structure of the combined graphene/MoS_2 nanocomposite is depicted in Fig. 1.

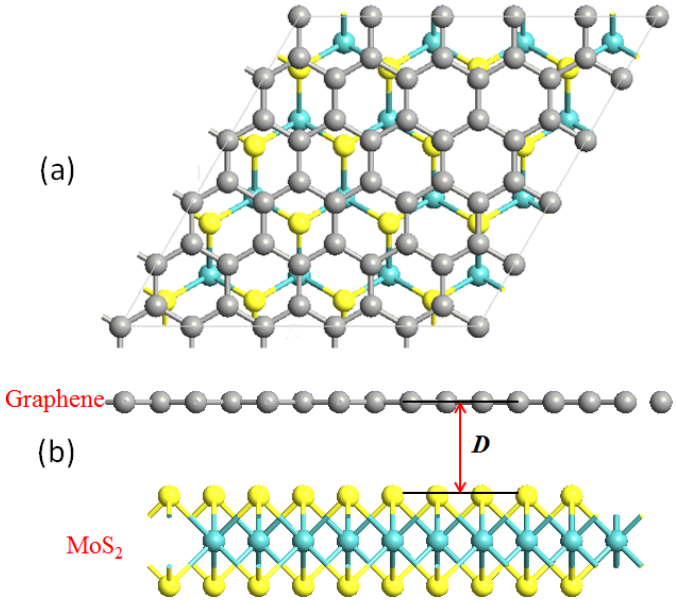

Fig. 1. (a) Top view and (b) side view of the relaxed atomic structures of the graphene/MoS_2 nanocomposite. D stands for the equilibrium interlayer distance between the graphene and the topmost S layer in the MoS_2 part.

The interlayer distance D between graphene and the topmost S layer of the MoS_2 part after the geometric optimization structure is obtained to be 3.43 Å. This value of the interlayer distance is comparable with that in other typical van der Waals (vdW) graphene-based nanocomposite, such as graphene/phosphorene (3.43 Å) [10], graphene/WS_2 (3.49 Å) [24], graphene/GaN (3.315 Å) [25] and so forth. It indicates that the graphene/MoS_2 nanocomposite is typical vdW system, where the weak vdW forces are mainly contributed. Furthermore, to check the structural stability of the graphene/MoS_2 nanocomposite, we calculate its binding energy as follows:

$$E_b = \frac{E_{nanocomposite} - E_{graphene} - E_{MoS_2}}{A} \quad (3)$$

Here, $E_{\text{nanocomposite}}$, E_{graphene}, and E_{MoS2}, respectively, are the total energies of the graphene/MoS_2 nanocomposite, isolated graphene and MoS_2 monolayer. A is the in-plane surface area of the nanocomposite. The calculated binding energy of the graphene/MoS_2 nanocomposite is calculated to be –8.29 meV/Å^2. The "-" sign of the binding energy demonstrates that the graphene/MoS_2 nanocomposite is stable at the ground state with the equilibrium interlayer distance of 3.43 Å. Thus, the weak vdW interactions dominate between graphene and MoS_2 layers, suggesting that MoS_2

material can be used as an ideal substrate for graphene with their intrinsic electronic structures undisturbed. Our obtained results are consistent with the calculated result for bilayer graphene [26].

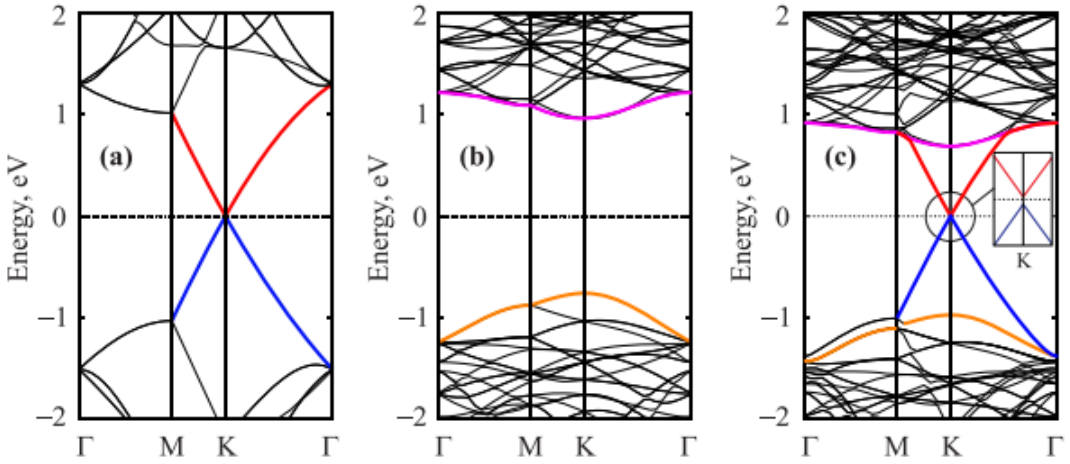

Fig. 2. Band structures of isolated (a) graphene (b) MoS_2 monolayers and (c) combined graphene/MoS_2 nanocomposite. The inset in Fig. 2(c) is the band gap, opened in the graphene at the Dirac K point.

The electronic band structures of the isolated graphene, MoS_2 monolayers and their graphene/MoS_2 nanocomposite are depicted in Fig. 2. One can observe from Fig. 2a that the graphene has a linear relation at the Dirac K point, resulting in the gap-less semiconductor. On the contrary, MoS_2 monolayer displays a direct band gap semiconductor, forming between the valence band maximum (VBM) and conduction band minimum (CBM) at the K Dirac point, as illustrated in Fig. 2b. When the graphene/MoS_2 nanocomposite is formed, one can clearly observe that its electronic band structure seems to be a combination of that of the individual constituent graphene and MoS_2 monolayers. It indicates that the electronic properties of both graphene and MoS_2 monolayers are well preserved in their combined graphene/MoS_2 nanocomposite. The Dirac cone at the K point of graphene is preserved in such nanocomposite, suggesting that its intrinsic electronic characteristics are maintained. More interestingly, we find that when the graphene/MoS_2 nanocomposite is formed, a tiny band gap of 10 meV has opened at the Dirac point of graphene, making it suitable for designing next-generation high speed optoelectronic nanodevices, such as field-effect transistor, as illustrated in Fig. 3. The mechanism of such band gap, opening in graphene is due to the symmetry breaking of the sublattice's graphene. This behavior was also confirmed by the experimental report [8, 27].

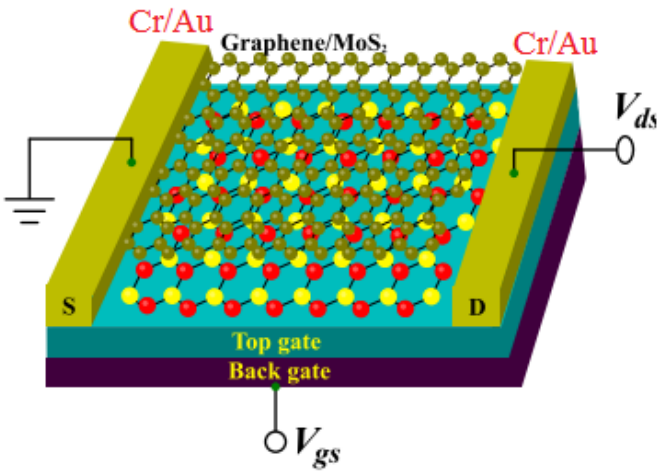

Fig. 3. Schematic model of field-effect transistor based on the graphene/MoS_2 nanocomposite.

More interestingly, when the graphene/MoS_2 nanocomposite is formed, it creates the metal/semiconductor contact, resulting in the formation of the Schottky or Ohmic contact. It should be noted that the performance of nanodevices depends on the formation of the Schottky or Ohmic contact in the metal/semiconductor contact. Depending of the position of the Fermi energy level, as depicted in Fig. 2c, we can find that the graphene/MoS_2 nanocomposite forms the Schottky contact. According to the Schottky-Mott rule [28], the Schottky barrier height of the n-type and p-type Schottky contact can be obtained as: $\Phi_{B,n} = E_F - E_{VBM}$, and $\Phi_{B,p} = E_{CBM} - E_F$, where E_{VBM}, E_{CBM} and E_F, respectively, are the positions of the VBM, the CBM and the Fermi level of the graphene/MoS_2 nanocomposite. Our calculated $\Phi_{B,n}$ the graphene/MoS_2 nanocomposite is 0.49 eV, which is slightly smaller than the $\Phi_{B,p}$ of 1.24 eV, indicating that the nanocomposite forms the n-type Schottky contact at the ground state. It should be noted that the Schottky contact in the graphene/MoS_2 nanocomposite is very different from traditional metal-semiconductor Schottky one. One is that graphene is adsorbed physically on MoS_2 monolayer without dangling bonds. In addition, the n-type Schottky barrier height of the graphene/MoS_2 nanocomposite is still smaller than that in other graphene-based nanocomposites, such as graphene/GaN [29], graphene/phosphorene [30]. It indicates that the Schottky devices based on the graphene/MoS_2 nanocomposite will predict to present a better performance than those based on the graphene/GaN and graphene/phosphorene.

Furthermore, the optical absorption of the nanocomposite is so crucial for the efficient utilization of the solar energy efficiency. We hence calculated the optical absorption spectra as a function of the photon energy. The optical absorption coefficient $\alpha(\omega)$ is calculated as follows:

$$\alpha(\varpi) = \sqrt{2}\varpi\left(\sqrt{\varepsilon_1^2(\varpi) + \varepsilon_2^2(\varpi)} - \varepsilon_1(\varpi)\right)^{\frac{1}{2}} \quad (4)$$

Here, $\varepsilon_1(\varpi)$ and $\varepsilon_2(\varpi)$ are the real and imaginary part of dielectric functions of materials.

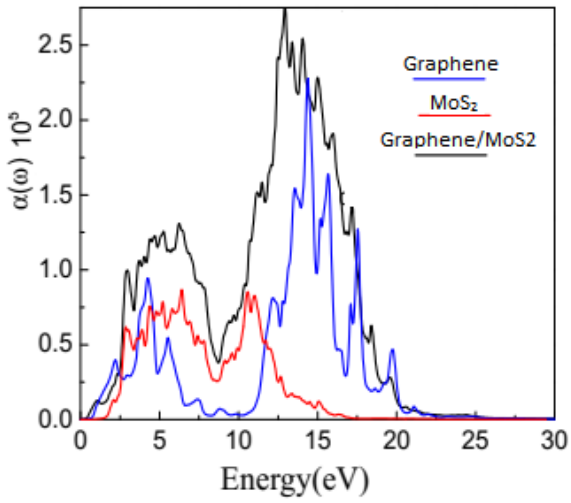

Fig. 4. Optical absorption of the graphene/MoS_2 nanocomposite.

The optical absorption coefficient of the graphene/MoS_2 nanocomposite is displayed in Fig. 4 along with that of the individual constituent graphene and MoS_2 monolayers. We can find that the graphene/MoS_2 nanocomposite exhibits a large absorption coefficient than the graphene and MoS_2 monolayers. The maximum of absorption intensity can reach up to 2.5×10^5 cm^{-1}. In addition, one can observe that the optical band gap of the graphene/MoS_2 nanocomposite is still smaller than that of the individual constituent graphene and MoS_2 monolayers. It is well-known that the optical absorption coefficient of MoS_2 is quite small, this leads to difficulties in the application of MoS_2 in optoelectronic devices. The formation of two-layer heterostructures based on MoS_2 to achieve a high absorption coefficient, as in the case of graphene/MoS_2, has brought new prospects for the application of MoS_2 in the optoelectronics.

We now turn to consider the mechanical properties of the graphene/MoS_2 nanocomposite. We first calculate the elastic stiffness constants C_{ij} by using the stress-strain relationship and the elastic moduli. As above-mentioned, the graphene/MoS_2 nanocomposite has the hexagonal structure, thus we further consider only the values of $C_{11} = C_{22}$, C_{12}, and C_{66} in the graphene/MoS_2 nanocomposite. The layer modulus of 2D system, including graphene/MoS_2 nanocomposite can be calculated as follows:

$$\gamma^{2D} = \frac{1}{2}\left[C_{11} + C_{12}\right]$$

From this point, the average Young's modulus (*E*), Poisson's ratio (υ) and shear modulus (G) can be calculated as follows:

$$E = \frac{C_{11}^2 - C_{12}^2}{C_{11}}; \upsilon = \frac{C_{12}}{C_{11}}; G = C_{66}$$

Tab. 2. Calculated elastic stiffness constants (N/m), Young's modulus (N/m), and Poisson's ratio of the graphene/MoS_2 nanocomposite along with those of isolated graphene and MoS_2 monolayers.

2D systems	C_{11}	C_{12}	C_{66}	Layer modulus	Young's modulus	Poisson's ratio
Graphene	356.3	62.3	150.5	209.3	345.4	0.17
MoS_2	131.2	39.2	46.3	85.2	119.5	0.34
Graphene/MoS_2 nanocomposite	512.3	113.4	200.3	312.85	487.2	0.22

One can observe from Tab. 2 that the elastic properties of the graphene/MoS_2 nanocomposite are enhanced in comparison with those of the constituent isolated graphene and MoS_2 monolayers. More interestingly, we can find that the elastic properties of such nanocomposite seem to be a combination of those of the constituent monolayers. Therefore, we can conclude that when the graphene stacked on the MoS_2 to form the graphene/MoS_2 nanocomposite, its elastic properties, including layer and Young's modulus are better than that of each individual monolayer, making it promising candidate for multifunctional nanodevices.

4. Conclusions

In conclusion, we have constructed an ultrathin graphene/MoS_2 nanocomposite and investigated its electronic, optical and mechanical properties using first principles calculations. We find that in the graphene/MoS_2 nanocomposite, the intrinsic properties of both graphene and MoS_2 layers are well preserved because of the weak vdW interactions, dominating between graphene and MoS_2 monolayers. The graphene/MoS_2 nanocomposite exhibits the enhanced electronic, optical and mechanical properties as compared with those of individual constituent graphene and MoS_2 monolayers. These findings provide an opportunity for the graphene/MoS_2 nanocomposite in the next-generation nanoelectronic and optoelectronic devices, which can be used to replace principal silicon-based devices.

Acknowledgements

This research is funded by the Vietnam National Foundation for Science and Technology Development (NAFOSTED) under grant number 103.01-2019.05.

References

1. K. S. Novoselov, A. K. Geim, S. V. Morozov, D. Jiang, Y. Zhang, S. V. Dubonos, I. V. Grigorieva, and A. A. Firsov (2004). Electric field effect in atomically thin carbon films. *Science, 306,* 666-669.
2. K. S. Novoselov, A. K. Geim, S. Morozov, D. Jiang, M. I. Katsnelson, I. Grigorieva, S. Dubonos, Firsov, and A. A. Firsov (2005). Two-dimensional gas of massless Dirac fermions in graphene. *Nature, 438,* 197.
3. F. Koppens, T. Mueller, P. Avouris, A. Ferrari, M. Vitiello, and M. Polini (2014). Photodetectors based on graphene, other two-dimensional materials and hybrid systems, *Nature Nanotechnology, 9,* 780.
4. C. Xie, C. Mak, X. Tao, and F. Yan (2017). Photodetectors based on two-dimensional layered materials beyond graphene. *Advanced Functional Materials, 27,* 1603886.
5. L. Li, Y. Yu, G. J. Ye, Q. Ge, X. Ou, H. Wu, D. Feng, X. H. Chen, and Y. Zhang (2014). Black phosphorus field-effect transistors. *Nature Nanotechnology, 9,* 372.
6. B. Qiu, X. Zhao, G. Hu, W. Yue, J. Ren, and X. Yuan (2018). Optical Properties of Graphene/MoS_2 Heterostructure: First Principles Calculations. *Nanomaterials, 8,* 962.
7. J.-W. Jiang and H. S. Park (2014). Mechanical properties of MoS_2/graphene heterostructures. *Applied Physics Letters, 105,* 033108.
8. Z. B. Aziza, H. Henck, D. Di Felice, D. Pierucci, J. Chaste, C. H. Naylor, A. Balan, Y. J. Dappe, A. C. Johnson, and A. Ouerghi (2016). Bandgap inhomogeneity of MoS_2 monolayer on epitaxial graphene bilayer in van der Waals p-n junction. *Carbon, 110,* 396-403.
9. N. N. Hieu, H. V. Phuc, V. V. Ilyasov, N. D. Chien, N. A. Poklonski, N. Van Hieu, and C. V. Nguyen (2017). First-principles study of the structural and electronic properties of graphene/MoS_2 interfaces. *Journal of Applied Physics, 122,* 104301.
10. W. Hu, T. Wang, and J. Yang (2015). Tunable Schottky contacts in hybrid graphene–phosphorene nanocomposites. *Journal of Materials Chemistry C, 3,* 4756-4761.
11. R. Lu, J. Liu, H. Luo, V. Chikan, and J. Z. Wu (2016). Graphene/GaSe-nanosheet hybrid: Towards high gain and fast photoresponse. *Scientific Reports, 6,* 19161.
12. H. Zeng, J. Zhao, A.-Q. Cheng, L. Zhang, Z. He, and R.-S. Chen (2018). Tuning electronic and optical properties of arsenene/C_3N van der Waals heterostructure by vertical strain and external electric field. *Nanotechnology, 29,* 075201.
13. Q. Zhang and U. Schwingenschlögl (2018). Rashba effect and enriched spin-valley coupling in Ga X/MX_2 (M = Mo, W; X = S, Se, Te) heterostructures. *Physical Review B, 97,* 155415.

14. P. Giannozzi, S. Baroni, N. Bonini, M. Calandra, R. Car, C. Cavazzoni, D. Ceresoli, G. L. Chiarotti, M. Cococcioni, and I. Dabo (2009). QUANTUM ESPRESSO: A modular and open-source software project for quantum simulations of materials. *Journal of Physics: Condensed Matter, 21*, 395502.
15. J. P. Perdew, K. Burke, and M. Ernzerhof (1996). Generalized gradient approximation made simple. *Physical Review Letters, 77*, 3865.
16. S. Grimme (2006). Semiempirical GGA-type density functional constructed with a long-range dispersion correction. *Journal of Computational Chemistry, 27*, 1787-1799.
17. I. V. Lebedeva, A. V. Lebedev, A. M. Popov, and A. A. Knizhnik (2017). Comparison of performance of van der Waals-corrected exchange-correlation functionals for interlayer interaction in graphene and hexagonal boron nitride. *Computational Materials Science, 128*, 45-58.
18. S. A. Tawfik, T. Gould, C. Stampfl, and M. J. Ford (2018). Evaluation of van der Waals density functionals for layered materials. *Physical Review Materials, 2*, 034005.
19. T. Björkman, A. Gulans, A. Krasheninnikov, and R. Nieminen (2012). Are we van der Waals ready? *Journal of Physics: Condensed Matter, 24*, 424218.
20. A. K. Geim and K. S. Novoselov (2007). The rise of graphene. *Nature Materials, 6*, 183-191.
21. J. A. Wilson and A. Yoffe (1969). The transition metal dichalcogenides discussion and interpretation of the observed optical, electrical and structural properties. *Advances in Physics, 18*, 193-335.
22. P. Johari and V. B. Shenoy (2012). Tuning the electronic properties of semiconducting transition metal dichalcogenides by applying mechanical strains. *ACS nano, 6*, 5449-5456.
23. A. C. Neto, F. Guinea, N. M. Peres, K.S. Novoselov, and A. K. Geim (2009). The electronic properties of graphene. *Reviews of Modern Physics, 81*, 109.
24. F. Zhang, W. Li, Y. Ma, Y. Tang, and X. Dai (2017). Tuning the Schottky contacts at the graphene/WS_2 interface by electric field. *RSC Advances, 7*, 29350-29356.
25. Z. Deng and X. Wang (2019). Strain engineering on the electronic states of two-dimensional GaN/graphene heterostructure. *RSC Advances, 9*, 26024-26029.
26. E. Mostaani, N. Drummond, and V. Fal'Ko (2015). Quantum Monte Carlo calculation of the binding energy of bilayer graphene. *Physical Review Letters, 115*, 115501.
27. D. Pierucci, H. Henck, J. Avila, A. Balan, C. H. Naylor, G. Patriarche, Y. J. Dappe, M. G. Silly, F. Sirotti, and A. C. Johnson (2016). Band alignment and minigaps in monolayer MoS_2-graphene van der Waals heterostructures. *Nano Letters, 16*, 4054-4061.
28. J. Bardeen (1947). Surface states and rectification at a metal semi-conductor contact. *Physical Review, 71*, 717.
29. M. Sun, J.-P. Chou, Q. Ren, Y. Zhao, J. Yu, and W. Tang (2017). Tunable Schottky barrier in van der Waals heterostructures of graphene and g-GaN. *Applied Physics Letters, 110*, 173105.
30. B. Liu, L.-J. Wu, Y.-Q. Zhao, L.-Z. Wang, and M.-Q. Caii (2016). Tuning the Schottky contacts in the phosphorene and graphene heterostructure by applying strain. *Physical Chemistry Chemical Physics, 18*, 19918-19925.

NGHIÊN CỨU CÁC TÍNH CHẤT ĐIỆN TỬ, QUANG HỌC VÀ CƠ TÍNH CỦA VẬT LIỆU NANO COMPOSITE GRAPHENE/MoS_2

Tóm tắt: *Trong bài báo này, chúng tôi mô phỏng và nghiên cứu các tính chất điện tử, quang học và cơ tính của hệ vật liệu màng mỏng nano graphene/MoS_2 sử dụng lý thuyết phiếm hàm mật độ. Kết quả nghiên cứu cho thấy lực tương tác yếu van der Waals giữa các lớp vật liệu giữ cho hệ vật liệu nanocomposite graphene/MoS_2 bền vững và không gây phá hủy các tính chất điện tử nổi trội của graphene và MoS_2 đơn lớp. Bên cạnh đó, chúng tôi thấy rằng các tính chất quang học và cơ tính của graphene và MoS_2 được tăng cường trong hệ vật liệu nanocomposite. Hệ số quang hấp thụ tối đa của hệ có thể đạt $2,5\times10^5$ cm^{-1}. Trong khi đó, mô đun đàn hồi Young của hệ nanocomposite này tăng lên tới 487,2 N/m^2. Các kết quả nghiên cứu này chỉ ra rằng sự hình thành hệ vật liệu màng mỏng nanocomposite của graphene và MoS_2 là phương pháp hiệu dụng để tăng cường các tính chất điện tử, quang học cũng như cơ tính của các vật liệu tiềm năng graphene và MoS_2.*

Từ khóa: Vật liệu nanocomposite graphene/MoS_2; các vật liệu hai chiều; phương pháp phiếm hàm mật độ.

Received: 10/02/2020; *Revised:* 26/7/2020; *Accepted for publication:* 28/7/2020

❑